



Since January 2020 Elsevier has created a COVID-19 resource centre with free information in English and Mandarin on the novel coronavirus COVID-19. The COVID-19 resource centre is hosted on Elsevier Connect, the company's public news and information website.

Elsevier hereby grants permission to make all its COVID-19-related research that is available on the COVID-19 resource centre - including this research content - immediately available in PubMed Central and other publicly funded repositories, such as the WHO COVID database with rights for unrestricted research re-use and analyses in any form or by any means with acknowledgement of the original source. These permissions are granted for free by Elsevier for as long as the COVID-19 resource centre remains active.

Characterizations of Coronavirus *cis*-Acting RNA Elements and the Transcription Step Affecting Its Transcription Efficiency

Sungwhan An* and Shinji Makino*†¹

*Department of Microbiology, and †Institute for Cellular and Molecular Biology, The University of Texas at Austin, Austin, Texas 78712-1095

Received November 14, 1997; returned to author for revision December 19, 1997; accepted January 26, 1998

Seven to eight species of viral subgenomic mRNAs are produced in coronavirus-infected cells. These mRNAs are produced in different quantities, and their molar ratios remain constant during viral replication. We studied RNA elements that affect coronavirus transcription efficiency by characterizing a series of cloned coronavirus mouse hepatitis virus (MHV) defective interfering (DI) RNAs containing an inserted intergenic sequence, from which subgenomic DI RNA is transcribed in MHV-infected cells. Certain combinations of upstream and downstream flanking sequences of the intergenic sequence suppressed subgenomic DI RNA transcription, yet changing one of the flanking sequences to a different sequence eliminated transcription suppression. The suppressive effect of certain combinations of flanking sequences, but not all combinations, could be counteracted by altering the intergenic sequence. Thus, the combination of intergenic sequence and flanking sequence affected transcription efficiency. We also characterized another set of DI RNAs designed to clarify which transcription step determines the relative molar ratios of coronavirus mRNAs. Our study indicated that if subgenomic mRNAs were exclusively synthesized from negative-strand genomic RNA, then the relative molar ratios of coronavirus mRNAs were most likely determined after synthesis of the genomic-sized template RNA. If negative-strand subgenomic RNAs were templates for subgenomic mRNAs, then the relative molar ratios of coronavirus mRNAs probably were determined after synthesis of the genomic-sized template RNA used for subgenomic-sized RNA transcription but prior to the completion of the synthesis of subgenomic-sized RNAs containing the leader sequence. The relative molar ratios of coronavirus mRNAs, therefore, seem to have been established prior to a putative replicon-type amplification of subgenomic mRNAs. © 1998

Academic Press

INTRODUCTION

Many eukaryotic RNA viruses express their gene(s) by producing subgenomic mRNA(s) in infected cells. Coronavirus, an enveloped virus containing a large positive-sense single-strand RNA, belongs to this group. Cells infected with mouse hepatitis virus (MHV), a prototypic coronavirus, produce seven to eight species of virus-specific mRNAs that make up a 3' coterminal nested set structure (Lai *et al.*, 1981; Leibowitz *et al.*, 1981). These mRNAs, which are named mRNAs 1 through 7 in decreasing order of size (Lai *et al.*, 1981; Leibowitz *et al.*, 1981), are produced in different quantities, and their molar ratios remain constant during MHV replication. The 5'-end of the MHV genomic RNA and the subgenomic mRNAs start with a leader sequence that is approximately 72 to 77 nucleotides (nt) long (Lai *et al.*, 1983, 1984; Spaan *et al.*, 1983); the presence of the leader sequence in subgenomic mRNAs is a unique characteristic in coronavirus and arterivirus (de Vries *et al.*, 1990), which is closely related to coronavirus. Curiously, on the genome, the leader sequence is not found any place besides the 5'-end, yet the subgenomic mRNAs have the

leader sequences fused with the mRNA body sequences. The mRNA body sequences begin from a UC-UAAAC transcription consensus sequence or a very similar sequence of intergenic sequences, which is located upstream of each MHV gene. Coronavirus transcription undergoes a discontinuous transcription step, in which the leader sequence somehow joins to the body of the subgenomic RNA (Jeong and Makino, 1994; Zhang *et al.*, 1994). Genomic-sized and subgenomic-sized negative-strand RNAs, each of which corresponds to one of the subgenomic mRNA species, are also present in coronavirus-infected cells (Sethna *et al.*, 1989). These negative-strand RNAs contain an antileader sequence at the 3'-end and a poly U sequence at the 5'-end (Sethna *et al.*, 1991).

Several models have been proposed to explain coronavirus subgenomic RNA synthesis. One model proposes that negative-strand RNA synthesis starts on genomic RNA and terminates at the intergenic sequence (Sawicki and Sawicki, 1990). In this model, the leader sequence joins to the body of subgenomic RNA either by relocalization of negative-strand subgenomic RNA to the leader sequence of the genomic RNA (antileader sequence joins to negative-strand subgenomic RNA), or during subgenomic mRNA synthesis on negative-strand subgenomic RNA template (Sawicki and Sawicki, 1990).

¹To whom correspondence and reprint requests should be addressed. Fax: (512) 471-7088. E-mail: makino@mail.utexas.edu.

Another way to envision negative-strand subgenomic RNA synthesis is provided by the idea that processing of the full-length negative-strand genomic RNA occurs after transcription from the genome. Subgenomic mRNA synthesis would follow processing of subgenomic negative strand RNAs; the leader sequence could join the body sequence during processing of negative-strand genomic RNA or during subgenomic mRNA synthesis on negative-strand subgenomic RNA. These two models propose that negative-strand subgenomic RNAs are synthesized prior to the synthesis of subgenomic mRNAs. All other transcription models propose that subgenomic mRNAs are synthesized prior to the synthesis of negative-strand subgenomic RNA. Subgenomic mRNAs may be synthesized by the processing of the positive-strand genomic RNA (Baric *et al.*, 1983), or by transcription from negative-strand genomic RNA by a unique leader-primed transcription mechanism, in which short "free" leader RNAs are used as primers for subgenomic mRNA synthesis (Baric *et al.*, 1983), or by polymerase jumping from leader sequence to intergenic sequence during subgenomic mRNA synthesis on the negative-strand genomic RNA template (Spaan *et al.*, 1983). In these models, once subgenomic mRNAs are synthesized, negative-strand subgenomic RNAs are copied on subgenomic mRNAs. Negative-strand subgenomic RNAs may have several different effects on transcription. These negative-strand subgenomic RNAs may be templates for subgenomic mRNA synthesis (Sawicki and Sawicki, 1990; Schaad and Baric, 1994), or may become replicons which undergo replication to amplify more subgenomic mRNA and negative-strand subgenomic RNAs (Sethna *et al.*, 1989). Alternatively, these negative-strand subgenomic RNAs may not participate in subsequent transcription; they may be dead-end transcription products (Jeong and Makino, 1992). All of the coronavirus transcription models postulate several transcription steps for the production of mature mRNAs: one of these unidentified transcription steps is that which defines the relative molar ratios of subgenomic mRNAs.

Due to the large size of coronavirus genomic RNA, a coronavirus infectious cDNA clone has not yet been constructed. Instead, for studying transcription we use coronavirus defective interfering (DI) RNAs that contain an inserted intergenic sequence from which transcription in DI RNA-replicating, coronavirus-infected cells yields a subgenomic DI RNA with a leader sequence (Makino *et al.*, 1991). Studies using MHV DI RNAs identified RNA elements that affect transcription (Jeong *et al.*, 1996; Joo and Makino, 1992, 1995; Makino and Joo, 1993; Makino *et al.*, 1991; van der Most *et al.*, 1994; van Marle *et al.*, 1995). One study showed that a series of DI RNAs, each of which contains a 0.4-kb-long sequence derived from various regions of the MHV sequence with an intergenic sequence in the middle, transcribe different amounts of subgenomic DI RNA (Jeong *et al.*, 1996),

demonstrating that sequences flanking the intergenic sequence affect transcription. Other studies showed that differences in the sequence of the inserted intergenic sequence also affect transcription (Jeong *et al.*, 1996; Joo and Makino, 1992; van der Most *et al.*, 1994). A DI RNA containing a 12-nt-long intergenic sequence (12-nt sequence) (UCUAAUCUAAAC) that is flanked by 0.2-kb-long sequences upstream and downstream of the genes 6–7 junction transcribes only a small amount of subgenomic DI RNA, while a DI RNA containing an 18-nt-long naturally occurring intergenic sequence at genes 6–7 (18-nt sequence) (AAUCUAAUCUAAACUUUA) in the place of the 12-nt sequence transcribes a significantly higher amount of subgenomic DI RNA (Jeong *et al.*, 1996), demonstrating that the 18-nt sequence overcomes the flanking sequence-mediated transcription suppression.

Among the many unanswered questions about coronavirus transcription regulation, we addressed the following three questions: (I) Does replacement of the 12-nt sequence with the 18-nt sequence in the intergenic sequence always overcome flanking sequence-mediated transcription suppression? (II) Does the presence of one of the flanking sequences or the presence of certain combinations of upstream and downstream flanking sequences suppress transcription? (III) During which step of transcription are the relative ratios of MHV mRNAs mainly determined?

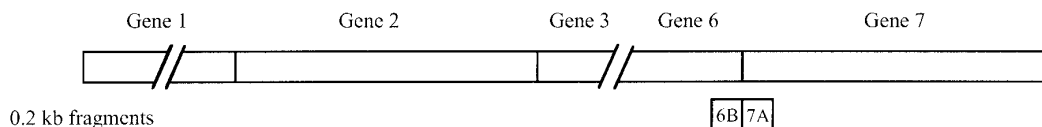
RESULTS

In an attempt to test for their susceptibility to transcription suppression by flanking sequences, the 18-nt or the 12-nt sequences were independently placed in the middle of different 0.4-kb sequences that had been inserted in a complete MHV DI ss cDNA clone, DE5-w3 (Makino and Lai, 1989b) between the *Afl*III site and the *Sac*II site (Fig. 1); this placement of the intergenic sequence resulted in its being flanked by two 0.2-kb sequences. We called the 0.2-kb-long regions that were located upstream and downstream of the intergenic sequence the 0.2-kb upstream flanking sequence and the 0.2-kb downstream flanking sequence, respectively.

Effect of 18-nt sequence on flanking sequence-mediated transcription suppression

The 18-nt sequence overcomes the effect of transcription suppression that the 0.2-kb upstream and downstream flanking sequences exert over the gene 6–7 intergenic sequence (Jeong *et al.*, 1996). We attempted to confirm this previous observation through a comparison of the transcripts (of *in vitro* synthesized DI RNA transfected into MHV-infected cells) from mutants FDI-6/7 M and FDI-6/7 wt, which both have 0.2-kb insertions upstream and downstream of the gene 6–7 intergenic sequence, and respectively carry the 12- and 18-nt sequence. Northern blot analysis of total cytoplasmic RNAs

MHV genomic RNA



DE5-w3 (DIssE)

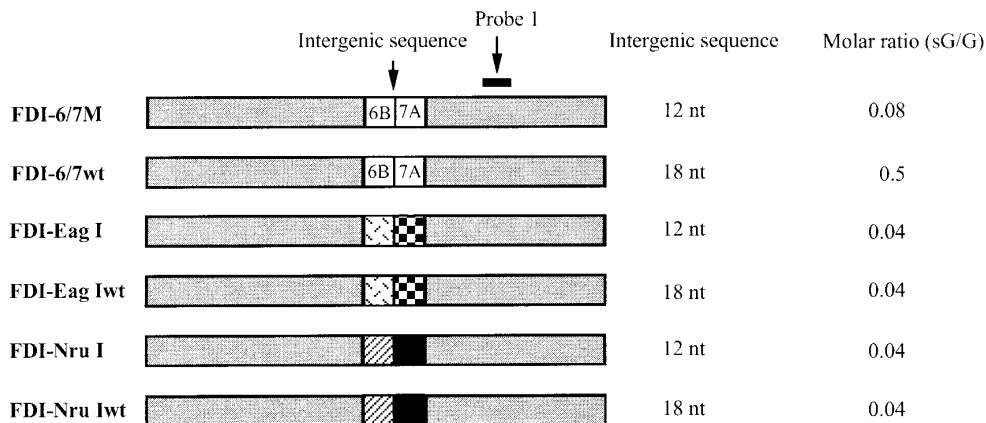
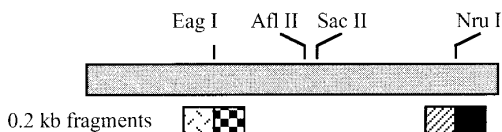


FIG. 1. Schematic diagram of the structure of MHV genomic RNA, DE5-w3, and DE5-w3-derived insertion mutants with flanking sequences. The 0.2-kb flanking sequences that were inserted into DE5-w3-derived insertion mutants are shown as 0.2-kb fragments. Each mutant has a 0.4-kb-long insertion between the *Afl*II site and *Sac*II site of DE5-w3. Molar ratio (sG/G) represents the average molar ratio of subgenomic DI RNA to genomic DI RNA from at least three independent experiments (see Fig. 2). The location of probe 1 used for Northern blot analysis (see Fig. 2) is also shown.

using probe 1, which corresponds to nucleotides 1488–1610 from the 5'-end DE5-w3, showed that FDI-6/7wt produced a significantly larger amount of subgenomic DI RNA than FDI-6/7 M (Fig. 2). These data were consistent with our previous result (Jeong *et al.*, 1996). As shown in Fig. 2 and subsequent figures, sometimes Northern blot analyses did not show a distinct MHV-A59 genomic RNA band; this was probably due to minor degradation of RNAs.

To examine whether replacement of the intergenic sequence from the 12-nt sequence to the 18-nt sequence always overcomes the flanking sequence-mediated transcription suppression, we examined two additional sets of DI RNAs; one set was FDI-*Eagl*wt and FDI-*Eagl*, and the other was FDI-*Nrul*wt and FDI-*Nrul*. FDI-*Eagl*wt and FDI-*Nrul*wt had an insertion of the 0.4-kb region surrounding the *Eagl* site and *Nrul* site of DE5-w3, respectively, and both contained the 18-nt sequence. (Fig. 1). FDI-*Eagl* and FDI-*Nrul* contain the 12-nt sequence in place of the 18-nt sequence (Jeong *et al.*, 1996). Northern blot analysis showed no significant differences in the

molar ratio of subgenomic DI RNA to genomic DI RNA among these four DI RNAs (Fig. 2). The replacement of the 12-nt sequence with the 18-nt sequence did not always overcome transcription suppression by the flanking sequences.

Characterization of transcription suppression mediated by flanking sequences

To know whether the presence of one of the flanking sequences or the presence of certain combinations of upstream and downstream flanking sequences suppress transcription, we constructed a series of DI RNAs, all of which contained the 12-nt sequence and had a different combination of the 0.2-kb upstream and downstream flanking sequences (Fig. 3). In these clones, one of the flanking sequences of FDI-*Eagl*, FDI-*Nrul*, and FDI-6/7 M was replaced with one of the 0.2-kb sequences that flank the naturally occurring intergenic sequences at genes 6–7, 2–3, and 1–2. Northern blot analysis using a 32 P-labeled probe 1 showed that all of the newly constructed

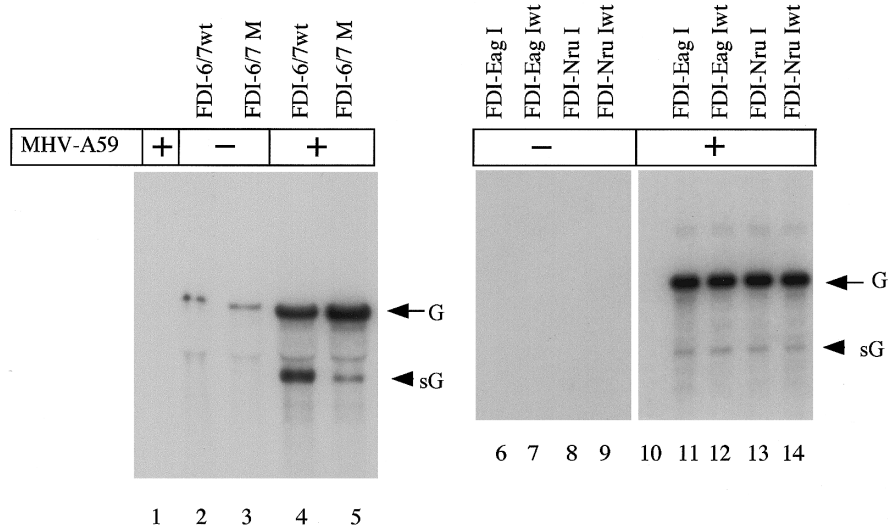


FIG. 2. Northern blot analysis of DE5-w3-derived insertion mutants. Intracellular RNAs were extracted from DI RNA-transfected, MHV-infected cells (lanes 4, 5, 11–14) or DI RNA-transfected, mock-infected cells (lanes 2, 3, 6–9). Lanes 1 and 10 represent RNA from MHV-infected cells. Total cytoplasmic RNAs (lanes 1–5) or poly(A)-containing RNAs (lanes 6–14) were analyzed by Northern blot analysis using probe 1 (see Fig. 1). Arrowhead and arrow point to subgenomic DI RNAs and genomic DI RNAs, respectively. The minute amount of genomic DI RNA-sized signal in lanes 2 and 3 represents the transfected DI RNA transcripts that were not degraded in MHV-uninfected cells.

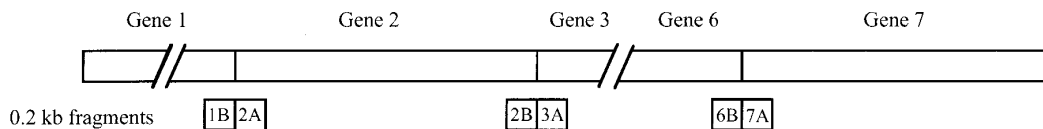
DI RNAs efficiently transcribed subgenomic DI RNA (Fig. 4). FDI-1/*Eagl* M, which had a naturally occurring 0.2-kb upstream flanking sequence at gene 1–2 plus a 0.2-kb downstream flanking sequence of the *Eagl* site, efficiently transcribed subgenomic DI RNA, while FDI-*Eagl* produced only a very low level of subgenomic DI RNA. These data may be interpreted as meaning that the 0.2-kb upstream flanking sequence of FDI-*Eagl* contained a transcription suppressive element(s). However, FDI-*Eagl*/2 M, which had the 0.2-kb upstream flanking sequence of FDI-*Eagl* and a 0.2-kb-long downstream flanking sequence at gene 1–2, efficiently transcribed subgenomic DI RNA; putative transcription suppressive element(s) at the 0.2-kb upstream flanking sequence did not suppress transcription. Comparison of FDI-*Eagl* and FDI-*Eagl*/2 M may indicate the presence of the transcription suppressive element(s) at the 0.2-kb downstream flanking sequence of the *Eagl* site. Again this putative transcription suppressive element(s) did not work at all in FDI-1/*Eagl*. These data indicated that the presence of either the 0.2-kb upstream or downstream flanking sequences of the *Eagl* site did not suppress transcription. Transcription suppression only occurred when the 0.2-kb upstream and downstream flanking sequences of FDI-*Eagl* were combined. Studies of the remaining two sets of DI RNAs resulted in the same conclusion; transcription suppression only occurred when the DI RNAs contained both upstream and downstream 0.2-kb fragments around the *Nrul* site and when DI RNA had both upstream and downstream 0.2-kb fragments at the gene 6–7 junction. In addition, we did not see any relationships between the transcription efficiency and the pres-

ence of a large open reading frame in subgenomic DI RNA among DI RNAs.

Transcription step that determined the molar ratio of subgenomic DI RNA to genomic DI RNA

For identification of the transcription step that mainly determines the relative molar ratios of MHV mRNAs, we first characterized constructs FDI-2/7 M and FDI-6/7 M (Fig. 5). They only differed from each other in their 0.2-kb upstream flanking sequence; FDI-2/7 M and FDI-6/7 M had 0.2-kb upstream flanking sequences from the upstream flanking sequences at genes 2–3 and genes 6–7, respectively (Fig. 5). In repeated experiments, the genomic DI RNA from the two DI RNAs (Figs. 4 and 6) replicated with very similar efficiencies. The difference between the subgenomic DI RNAs of FDI-6/7 M and FDI-2/7 M, however, was striking; FDI-6/7 M subgenomic DI RNA was significantly lower than FDI-2/7 M subgenomic DI RNA (Figs. 4 and 6). The structures of the subgenomic DI RNAs of both DI RNAs were expected to be the same, because both DI RNAs had the 12-nt sequence and had the same 0.2-kb downstream flanking sequence. Sequence analysis of cloned RT-PCR products of subgenomic DI RNA showed that both subgenomic DI RNAs had the helper MHV-derived leader sequence and the same leader–body fusion site (data not shown); the difference between the leader sequences of FDI-6/7 M and FDI-2/7 M and that of helper virus allowed for the identification of the origin of leader sequence in the subgenomic DI RNA. These data demonstrated that the subgenomic DI RNAs of both DI RNAs indeed had the same structure.

MHV genomic RNA



DE5-w3 (DIssE)

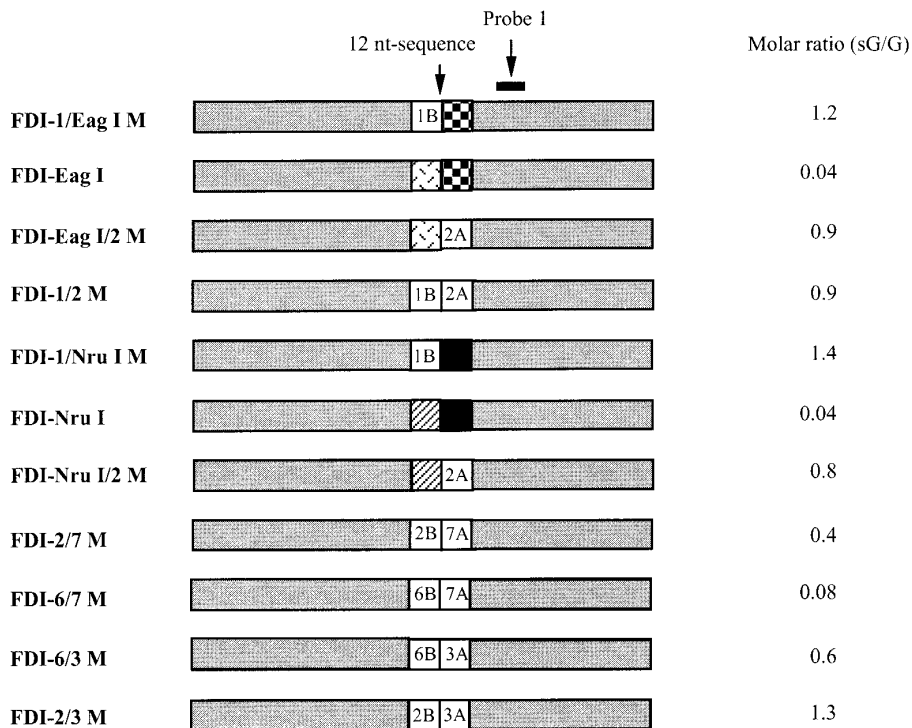


FIG. 3. Schematic diagram of the structure of MHV genomic RNA, DE5-w3, and DE5-w3-derived insertion mutants with flanking sequences. The 0.2-kb flanking sequences that were inserted into DE5-w3-derived insertion mutants are shown as 0.2-kb fragments. All mutants contained the 12-nt sequence in the middle of the inserted sequence. Molar ratio (sG/G) represents the average molar ratio of subgenomic DI RNA to genomic DI RNA from at least three independent experiments (see Fig. 4). The location of probe 1 used for Northern blot analysis (see Fig. 4) is also shown.

These data indicated that the molar ratio of subgenomic DI RNA to genomic DI RNA was determined at a transcription step(s) that occurred prior to or concomitant with the synthesis of subgenomic-sized DI RNA (of either polarity) containing leader sequence. The following are the logical bases for the previous statement: (I) The similar replication efficiencies of FDI-6/7 M and FDI-2/7 M indicated that similar amounts of helper virus-derived and host-derived factors were available for DI RNA synthesis of both constructs. (II) Efficiency of putative RNA synthesis from subgenomic-sized DI RNA template containing leader sequence of those identical subgenomic DI RNA probably is the same whether they were positive-stranded, negative-stranded, or both. If sub-

genomic DI RNAs accumulate by replicon-type amplification (Sethna *et al.*, 1989), then these subgenomic DI RNAs with identical structures probably amplify with the same efficiency. Any difference in the subgenomic to genomic DI RNA molar ratios of the two DI RNAs, therefore, should occur prior to a possible replicon-type amplification.

One of the transcription steps that possibly determines the ratio of subgenomic DI RNA to genomic DI RNA is the step that synthesizes biologically functional genomic-sized template RNA; genomic-sized template RNA may be either positive-stranded or negative-stranded. FDI-6/7 M might have produced significantly less genomic-sized transcription-template RNA than did

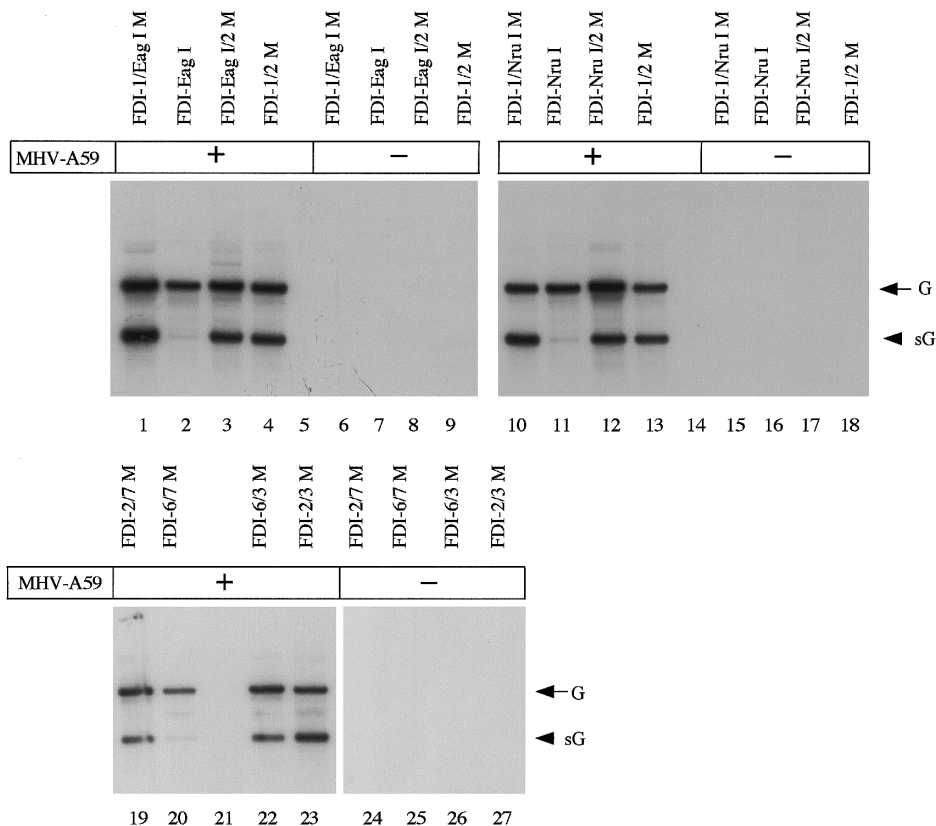


FIG. 4. Northern blot analysis of insertion mutants. Intracellular RNAs were extracted from DI RNA-transfected, MHV-infected cells (lanes 1–4, 10–13, 19, 20, 22, 23) or DI RNA-transfected, mock-infected cells (lanes 6–9, 15–18, 24–27). Lanes 5, 14, and 21 represent RNA from MHV-infected cells. Poly(A)-containing RNAs were analyzed by Northern blot analysis using probe 1 (see Fig. 1). Arrowhead and arrow point to subgenomic DI RNAs and genomic DI RNAs, respectively.

FDI-2/7 M; the sequence differences at the upstream flanking sequence of these two DI RNAs may be responsible for the differences in the amounts of biologically active template. Quantitative comparison of negative-strand or positive-strand DI genomic RNA of FDI-6/7 M and FDI-2/3 M may not reveal the difference in the amount of biologically functional template; both DI RNAs produced similar amounts of positive-strand DI genomic RNA (Figs. 4 and 6) and may produce similar amounts of negative-strand DI genomic RNAs, yet the amount of biologically functional genomic-sized template RNA that is used for transcription may differ between the two DI RNAs.

To examine whether FDI-6/7 M and FDI-2/7 M synthesized different amounts of genomic-sized RNA templates that function for transcription, we constructed and characterized FDI-2/7 M-dIG and FDI-6/7 M-dIG (Fig. 5). FDI-2/7 M-dIG and FDI-6/7 M-dIG each had an additional 12-nt sequence located 0.2 kb downstream of the 12-nt sequences of FDI-2/7 M and FDI-6/7 M, respectively. From these constructs, we expected synthesis of a large subgenomic DI RNA from the upstream 12-nt sequence and a small subgenomic DI RNA from the downstream 12-nt sequence. If FDI-6/7 M-dIG and FDI-2/7 M-dIG

replicated at similar efficiencies, and if the molar ratios of their genomic DI RNAs to their large subgenomic DI RNAs were respectively similar to those of their parent constructs, then regulation of the synthesis of the large subgenomic DI RNA in FDI-2/7 M-dIG and FDI-6/7 M-dIG is probably similar to regulation of subgenomic DI RNA synthesis in their individual parents. Along this line, if one parental construct produced fewer functioning genomic-sized RNA templates than the other parent, we expected that the successor constructs would likewise be related. In this case, FDI-6/7 M-dIG would produce less small subgenomic DI RNA than FDI-2/7 M-dIG, because FDI-6/7 M-dIG would have fewer genomic-sized template RNAs than the corresponding RNA of FDI-2/7 M-dIG. If the number of templates of FDI-2/7 M-dIG and FDI-6/7 M-dIG are similar, then similar amounts of small subgenomic DI RNA should be synthesized in FDI-2/7 M-dIG- and FDI-6/7 M-dIG-replicating cells.

Northern blot analysis using probe 2, which corresponds to nucleotides 1235–1491 from the 5'-end of DE5-w3, demonstrated replication of FDI-2/7 M-dIG and FDI-6/7 M-dIG (Fig. 6). Although FDI-6/7 M-dIG replicated slightly better than FDI-2/7 M-dIG in Fig. 6, this was not always the case; in other experiments, FDI-2/7 M-dIG

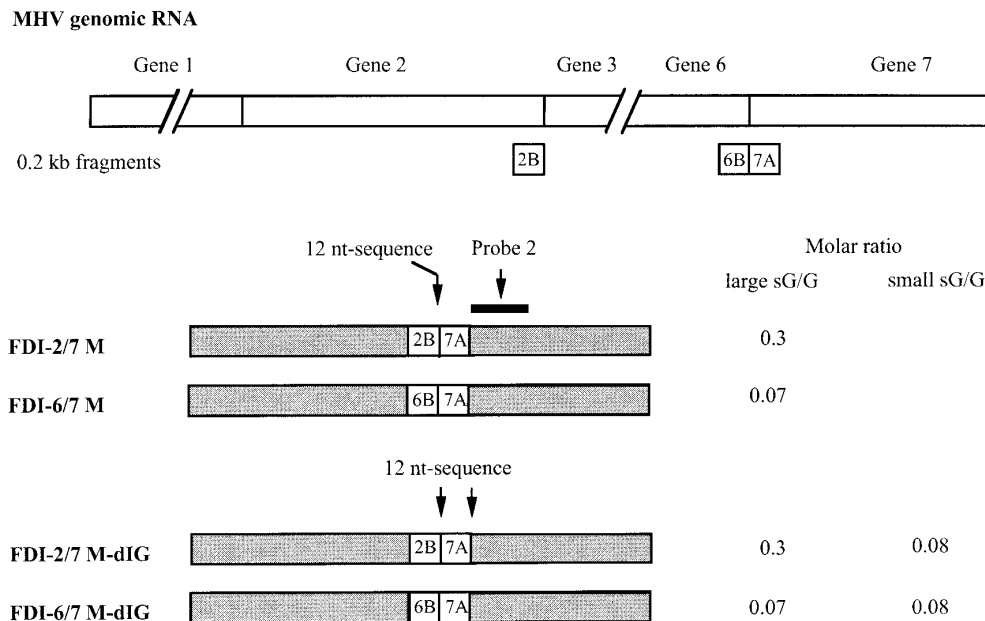


FIG. 5. Schematic diagram of the structure of insertion mutants. The 0.2-kb flanking sequences that were inserted into insertion mutants are shown as 0.2-kb fragments. Locations of the 12-nt sequence are also shown. Molar ratio represents the average molar ratio of subgenomic DI RNA to genomic DI RNA from at least three independent experiments (see Fig. 6). The molar ratios of subgenomic DI RNA to genomic DI RNA in FDI-2/7 M and in FDI-6/7 M, and that of large subgenomic DI RNA to genomic DI RNA in FDI-2/7 M-dIG and in FDI-6/7 M-dIG, are shown as large sG/G. The molar ratios of small subgenomic DI RNA to genomic DI RNA in FDI-2/7 M-dIG and in FDI-6/7 M-dIG are shown as small sG/G. The location of probe 2 used for Northern blot analysis (see Fig. 6) is also shown.

replicated slightly better than FDI-6/7 M-dIG. The average replication efficiencies of these two DI RNAs were very similar. The molar ratio of large subgenomic DI RNA to genomic DI RNA in FDI-2/7 M-dIG and that in FDI-6/7 M-dIG was comparable to that of subgenomic DI RNA to genomic DI RNA in FDI-2/7 M and FDI-6/7 M, respectively, indicating that transcription regulation in FDI-2/7 M-dIG and in FDI-6/7 M-dIG was the same or very similar to that in their respective parental constructs. Interestingly, the molar ratio of the small subgenomic DI RNA to genomic DI RNA in FDI-2/7 M-dIG and that in FDI-6/7 M-dIG was very similar. These data strongly indicated that the amount of biologically functional genomic-sized DI RNA template that is used for subgenomic-sized DI RNA transcription is similar in FDI-2/7 M-dIG and FDI-6/7 M-dIG.

The data indicated that these differences in the molar ratios of subgenomic DI RNA to genomic DI RNA most probably were set after the synthesis of genomic-sized template DI RNA. If coronavirus subgenomic mRNAs are synthesized exclusively from negative-strand genomic RNA, differences in the molar ratios of subgenomic DI RNA to genomic DI RNA should have been determined after the synthesis of genomic-sized template DI RNA. If subgenomic-sized negative-strand RNAs are templates for subgenomic mRNAs, then the molar ratios of subgenomic DI RNA to genomic DI RNA should have been determined after the synthesis of genomic-sized template DI RNA that is used for subgenomic-sized DI RNA

transcription but prior to the completion of the synthesis of subgenomic-sized DI RNAs containing the leader sequence.

DISCUSSION

Coronavirus transcription regulation and intergenic sequence/flanking sequence combinations

An earlier study demonstrated that certain MHV sequences that flank an inserted intergenic sequence suppress subgenomic DI RNA transcription (Jeong *et al.*, 1996). The present study showed that transcription suppression only occurred with certain combinations of upstream and downstream flanking sequences. No single flanking sequence showed dominant transcription suppression. These data suggested that both upstream and downstream flanking sequences affect transcription efficiency. An alternative interpretation may be that some flanking sequences, e.g., flanking sequences at genes 1–2 and 2–3 (see Figs. 3 and 4), have a dominant transcription enhancing element(s) that overcomes the suppressive effect caused by other flanking sequences, e.g., 0.4-kb sequences at the genes 6–7 junction, the *Eagl* site, and the *Nrul* site. We also showed that changing the intergenic sequence from a 12-nt sequence to an 18-nt sequence did not always overcome flanking sequence-mediated transcription suppression. Because changing from a 12-nt sequence to an 18-nt sequence increases the extent of base pairing between the 3'-region of

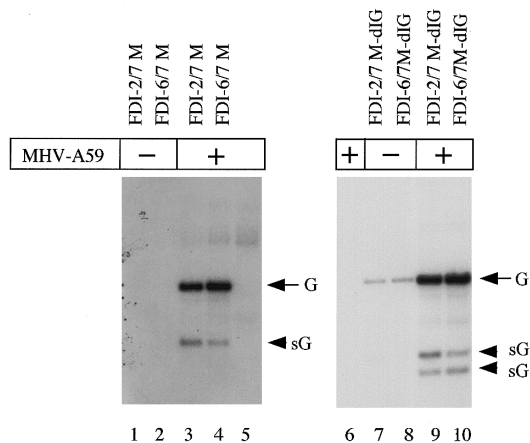


FIG. 6. Northern blot analysis of insertion mutants. Intracellular RNAs were extracted from DI RNA-transfected, MHV-infected cells (lanes 3, 4, 9, 10) or DI RNA-transfected, mock-infected cells (lanes 1, 2, 7, 8). Lanes 5 and 6 represent RNA from MHV-infected cells. Poly(A)-containing RNAs were analyzed by Northern blot analysis using probe 2 (see Fig. 5). Arrowhead and arrow point to subgenomic DI RNAs and genomic DI RNAs, respectively. The minute amount of genomic DI RNA-sized signal in lanes 7 and 8 represents the transfected DI RNA transcripts that were not degraded in MHV-uninfected cells.

leader sequence and the sequence at the intergenic sequence, these data were consistent with the previous finding that the extent of base pairing between the leader sequence and the intergenic sequence does not directly correlate with transcription efficiency (Joo and Makino, 1992; van der Most *et al.*, 1994). Our data indicated that the combination of the intergenic sequence with its upstream and downstream flanking sequences affected transcription efficiency. Probably an RNA structure assembled from these regions is important for the efficiency of transcription.

Other studies indicated that some MHV sequences in addition to the intergenic sequence and its flanking sequences also affect coronavirus transcription. We showed that the number of UCUAA repeats at the 3'-end of the leader sequence regulates the synthesis of certain mRNA species (Makino and Lai, 1989a; Shieh *et al.*, 1989). Lai and his colleagues showed that in MHV-infected cells, expression (Liao and Lai, 1994) or transfection (Lin *et al.*, 1994, 1996) of a positive-strand MHV DI RNA fragment that contains an inserted intergenic sequence and that lacks one part of the DI RNA *cis*-acting replication signals (Kim *et al.*, 1993; Kim and Makino, 1995; Lin and Lai, 1993) results in transcription of subgenomic DI RNA. Deletion analyses of these DI RNA fragments indicates involvement of the 5' and 3' regions in transcription (Liao and Lai, 1994; Lin *et al.*, 1994, 1996). Fischer *et al.* (1997) showed that a novel MHV subgenomic mRNA, which was very similar in size to MHV mRNA 4, is synthesized in cells infected with a recombinant MHV, which has a non-MHV sequence in place of gene 4. Interestingly, this recombinant MHV lacks a tran-

scription consensus sequence for this novel mRNA. These data indicate that formation of a higher-order RNA structure, assembled from several MHV RNA regions, is important for transcription. Furthermore, viral proteins as well as host-derived protein(s) are probably involved in formation of this higher-order RNA structure (Furuya and Lai, 1993).

If a higher-order RNA structure that is made by the 5'- and 3'-regions of the genome and an intergenic sequence with its flanking sequences is important for coronavirus transcription, then probably MHV DI RNA does not form the same structure; the MHV DI RNAs that we used for these experiments lack most of the MHV sequence and contain arbitrarily located intergenic sequence(s). We assume that DI RNA also forms a higher-order RNA structure, but the structure may be more suitable for RNA replication than for transcription. This possible difference in the higher-order RNA structures between MHV DI RNA and infectious MHV may be responsible for the poor transcription in MHV DI RNA; the molar ratio of mRNA 7 to mRNA 1 is about 100 (Leibowitz *et al.*, 1981), yet that of subgenomic DI RNA to genomic DI RNA containing intergenic sequence and flanking sequences at genes 6-7 is about 0.8 (Makino *et al.*, 1991).

The data from this study will be useful for the development of coronavirus-based expression vectors, in which multiple foreign genes may be expressed through subgenomic mRNAs of genetically engineered coronaviruses or coronavirus DI RNAs. There is a possibility that only a low level of subgenomic mRNA or subgenomic DI RNA will be synthesized in coronavirus expression vectors; a low level of transcription may result from insertion of a foreign gene downstream of the intergenic sequence. If this happens, as shown in this study, changing the 0.2-kb-long upstream flanking sequence to a different sequence, e.g., a naturally occurring upstream flanking sequence at genes 1-2 or at 2-3, may increase transcription efficiency.

The transcription step that determines the molar ratio of subgenomic DI RNA to genomic DI RNA

Based on our characterization of the two sets of DI RNAs shown in Fig. 6, we could not specify a coronavirus transcription step that determines the relative ratios of MHV mRNAs, but we can now better conceive of what those steps may be. If subgenomic mRNAs are synthesized prior to negative-strand subgenomic-sized RNA synthesis, then they are synthesized by leader-primed transcription, processing of positive-strand genomic RNA, or polymerase jumping from the leader to intergenic sequence. In leader-primed transcription and polymerase jumping mechanisms, the step that determines the relative molar ratios of mRNAs is likely to be the leader-body fusion step. If subgenomic mRNAs are syn-

thesized by the processing of precursor RNAs, then the relative molar ratios of mRNAs are determined either by the efficiency of RNA cleavage or the efficiency leader-body fusion or both. If the subgenomic-sized negative-strand RNAs are synthesized prior to the subgenomic mRNAs (Sawicki and Sawicki, 1990), then the efficiency of subgenomic-sized negative-strand RNA synthesis may determine the relative ratios of subgenomic mRNAs; the efficiency of subgenomic-sized negative-strand RNA synthesis may be determined by the efficiency of transcription termination at the intergenic sequence, the efficiency of relocalization of negative-strand subgenomic RNA lacking the antileader sequence to leader sequence of genomic-sized template RNA, or the efficiency of the processing of genomic-sized negative-strand RNA to subgenomic-sized RNAs. If subgenomic mRNA is synthesized on subgenomic-sized negative-strand RNA lacking the antileader sequence by priming of leader RNA, the efficiency of leader RNA priming may determine the relative molar ratios of subgenomic mRNAs.

The effect of double intergenic sequence insertion on subgenomic DI RNA transcription is described (Joo and Makino, 1995; van Marle *et al.*, 1995). We showed that transcription from an upstream intergenic sequence is strongly inhibited by the presence of a proximate downstream intergenic sequence (Joo and Makino, 1995). van Marle *et al.* (1995) described that transcription from upstream intergenic sequence is suppressed when two intergenic sequences are separated more than 300 nt. As shown in the present study, the molar ratio of large subgenomic DI RNA to genomic in FDI-2/7 M-dIG was similar to that of genomic DI RNA to subgenomic DI RNA in FDI-2/7 M. The same was the case with FDI-6/7 M-dIG and FDI-6/7 M. Insertion of an additional 12-nt sequence at a location 0.2 kb downstream from the 12-nt sequence did not significantly suppress transcription from the upstream 12-nt sequence, which was inconsistent with the data shown by van Marle *et al.* (1995). Our data may indicate that transcription suppression caused by the presence of downstream flanking sequence that is located far away from the upstream intergenic sequence occurs in certain DI RNAs, but is not a common property of coronavirus transcription in general.

MATERIALS AND METHODS

Virus and cells

The plaque-cloned A59 strain of MHV (Lai *et al.*, 1981) was used as a helper virus. DBT cells (Hirano *et al.*, 1974) were used for growth of virus and RNA transfection.

DNA construction

Recombinant PCR was used to create various insertions, as described previously (Higuchi, 1990). The same PCR condition was used for all cDNA construction. Plas-

mid DNA or MHV-JHM cDNA and primers were mixed in a PCR buffer containing 0.05 M KCl, 0.01 M Tris-HCl (pH 8.3), 0.0025 M MgCl₂, 0.01% gelatin, 0.17 mM each dNTPs and 5 U *Taq* polymerase (Promega). The sample was initially incubated at 94°C for 5 min and then incubated at 94°C for 1 min, 42°C for 1 min, and 72°C for 1 min, and that incubation was repeated for 30 cycles. A complete MHV DI_{SS}E cDNA clone, DE5-w3 (Makino and Lai, 1989b), was used as a parental clone for DNA construction. We obtained two 0.2-kb-long PCR products, each of which had either the 12-nt sequence or the 18-nt sequence at its end, by incubating the MHV-JHM cDNA or cloned MHV DI cDNA with two specific primers, one of which contained either the 12-nt or 18-nt sequence. The two purified PCR products made from each template were mixed, and the second PCR yielded a 0.4-kb-long product that had either the 12-nt sequence or the 18-nt sequence in its middle. The final PCR product was inserted into the *Afl*III site and *Sac*II site of DE5-w3 to produce the DI cDNAs used in the present study (Fig. 1). For all of the constructs, we sequenced the inserts that were derived from the PCR products to confirm the presence of specific sequences and the absence of extraneous mutations.

RNA transcription and transfection

Plasmid DNAs were linearized by *Xba*I digestion and transcribed with T7 RNA polymerase as previously described (Makino and Lai, 1989b). DI RNA synthesized *in vitro* was transfected into DBT cells that had been infected with MHV 1 h prior to infection. Lipofection (Makino *et al.*, 1991) was used for RNA transfection.

Preparation of virus-specific intracellular RNA and northern (RNA) blotting

Accumulation of intracellular DI RNAs were examined in MHV-infected, DI RNA-transfected cells. Intracellular RNAs from MHV-mock-infected, DI RNA-transfected cells and those from MHV-infected cells were used as controls. Intracellular RNAs were extracted at 7 h after MHV infection (Makino *et al.*, 1984). In most of the experiments, poly(A)-containing RNAs were collected by oligo(dT) column chromatography and characterized. Intracellular RNAs were denatured and electrophoresed through a 1% agarose gel containing formaldehyde and transferred onto nylon filters (Makino *et al.*, 1991). Northern blot hybridization was performed with a ³²P-labeled random-primed probe (Jeong and Makino, 1992). Radioactivity of individual RNA bands was determined by phosphorimaging analysis (Molecular Dynamics) of the membranes.

ACKNOWLEDGMENTS

The authors want to thank Sangeeta Banerjee for careful proofreading of the manuscript. This work was supported by Public Health Service Grants AI29984 and AI32591 from the National Institutes of Health.

REFERENCES

- Baric, R. S., Stohlman, S. A., and Lai, M. M. C. (1983). Characterization of replicative intermediate RNA of mouse hepatitis virus: Presence of leader RNA sequences on nascent chains. *J. Virol.* **48**, 633–640.
- de Vries, A. A. F., Chirnside, E. D., Bredenbeek, P. J., Gravestien, L. A., Horzinek, M. C., and Spaan, W. J. M. (1990). All subgenomic mRNAs of equine arteritis virus contain a common leader sequence. *Nucleic Acids Res.* **18**, 3241–3247.
- Fischer, F., Stegen, C. F., Koetzner, C. A., and Masters, P. S. (1997). Analysis of a recombinant mouse hepatitis virus expressing a foreign gene reveals a novel aspect of coronavirus transcription. *J. Virol.* **71**, 5148–5160.
- Furuya, T., and Lai, M. M. C. (1993). Three different cellular proteins bind to complementary sites on the 5'-end-positive and 3'-end-negative strands of mouse hepatitis virus RNA. *J. Virol.* **67**, 7215–7222.
- Higuchi, R. (1990). Recombinant PCR. In "PCR Protocols" (M. A. Innis, D. H. Gelfand, J. J. Sninsky, and T. J. White, Eds.), pp. 177–183. Academic Press, San Diego.
- Hirano, N., Fujiwara, K., Hino, S., and Matsumoto, M. (1974). Replication and plaque formation of mouse hepatitis virus (MHV-2) in mouse cell line DBT culture. *Arch. Gesamte. Virusforsch.* **44**, 298–302.
- Jeong, Y. S., and Makino, S. (1992). Mechanism of coronavirus transcription: Duration of primary transcription initiation activity and effect of subgenomic RNA transcription on RNA replication. *J. Virol.* **66**, 3339–3346.
- Jeong, Y. S., and Makino, S. (1994). Evidence for coronavirus discontinuous transcription. *J. Virol.* **68**, 2615–2623.
- Jeong, Y. S., Repass, J. F., Kim, Y.-N., Hwang, S. M., and Makino, S. (1996). Coronavirus transcription mediated by sequences flanking the transcription consensus sequence. *Virology* **217**, 311–322.
- Joo, M., and Makino, S. (1992). Mutagenic analysis of the coronavirus intergenic consensus sequence. *J. Virol.* **66**, 6330–6337.
- Joo, M., and Makino, S. (1995). The effect of two closely inserted transcription consensus sequences on coronavirus transcription. *J. Virol.* **69**, 272–280.
- Kim, Y.-N., Jeong, Y. S., and Makino, S. (1993). Analysis of *cis*-acting sequences essential for coronavirus defective interfering RNA replication. *Virology* **197**, 53–63.
- Kim, Y.-N., and Makino, S. (1995). Characterization of a murine coronavirus defective interfering RNA internal *cis*-acting replication signal. *J. Virol.* **69**, 4963–4971.
- Lai, M. M. C., Baric, R. S., Brayton, P. R., and Stohlman, S. A. (1984). Characterization of leader RNA sequences on the virion and mRNAs of mouse hepatitis virus, a cytoplasmic RNA virus. *Proc. Natl. Acad. Sci. USA* **81**, 3626–3630.
- Lai, M. M. C., Brayton, P. R., Armen, R. C., Patton, C. D., Pugh, C., and Stohlman, S. A. (1981). Mouse hepatitis virus A59: mRNA structure and genetic localization of the sequence divergence from hepatotropic strain MHV-3. *J. Virol.* **39**, 823–834.
- Lai, M. M. C., Patton, C. D., Baric, R. S., and Stohlman, S. A. (1983). Presence of leader sequences in the mRNA of mouse hepatitis virus. *J. Virol.* **46**, 1027–1033.
- Leibowitz, J. L., Wilhelmsen, K. C., and Bond, C. W. (1981). The virus-specific intracellular RNA species of two murine coronaviruses: MHV-A59 and MHV-JHM. *Virology* **114**, 39–51.
- Liao, C.-L., and Lai, M. M. C. (1994). Requirement of the 5'-end genomic sequence as an upstream *cis*-acting element for coronavirus subgenomic mRNA transcription. *J. Virol.* **68**, 4727–4737.
- Lin, Y.-J., and Lai, M. M. C. (1993). Deletion mapping of a mouse hepatitis virus defective interfering RNA reveals the requirement of an internal and discontinuous sequence for replication. *J. Virol.* **67**, 6110–6118.
- Lin, Y.-J., Liao, C.-L., and Lai, M. M. C. (1994). Identification of the *cis*-acting signal for minus-strand RNA synthesis of a murine coronavirus: Implication for the role of minus-strand RNA in RNA replication and transcription. *J. Virol.* **68**, 8131–8140.
- Lin, Y.-J., Zhang, X., Wu, R.-C., and Lai, M. M. C. (1996). The 3' untranslated region of coronavirus RNA is required for subgenomic mRNA transcription from a defective interfering RNA. *J. Virol.* **70**, 7236–7240.
- Makino, S., and Joo, M. (1993). Effect of intergenic consensus sequence flanking sequences on coronavirus transcription. *J. Virol.* **67**, 3304–3311.
- Makino, S., Joo, M., and Makino, J. K. (1991). A system for study of coronavirus mRNA synthesis: A regulated, expressed subgenomic defective interfering RNA results from intergenic site insertion. *J. Virol.* **65**, 6031–6041.
- Makino, S., and Lai, M. M. C. (1989a). Evolution of the 5'-end of genomic RNA of murine coronaviruses during passages *in vitro*. *Virology* **169**, 227–232.
- Makino, S., and Lai, M. M. C. (1989b). High-frequency leader sequence switching during coronavirus defective interfering RNA replication. *J. Virol.* **63**, 5285–5292.
- Makino, S., Taguchi, F., Hirano, N., and Fujiwara, K. (1984). Analysis of genomic and intracellular viral RNAs of small plaque mutants of mouse hepatitis virus, JHM strain. *Virology* **139**, 138–151.
- Sawicki, S. G., and Sawicki, D. L. (1990). Coronavirus transcription: Subgenomic mouse hepatitis virus replicative intermediates function in RNA synthesis. *J. Virol.* **64**, 1050–1056.
- Schaad, M. C., and Baric, R. S. (1994). Genetics of mouse hepatitis virus transcription: Evidence that subgenomic negative strands are functional templates. *J. Virol.* **68**, 8169–8179.
- Sethna, P. B., Hofmann, M. A., and Brian, D. A. (1991). Minus-strand copies of replicating coronavirus mRNAs contain antileaders. *J. Virol.* **65**, 320–325.
- Sethna, P. B., Hung, S.-L., and Brian, D. A. (1989). Coronavirus subgenomic minus-strand RNAs and the potential for mRNA replicons. *Proc. Natl. Acad. Sci. USA* **86**, 5626–5630.
- Shieh, C.-K., Lee, H.-J., Yokomori, K., La Monica, N., Makino, S., and Lai, M. M. C. (1989). Identification of a new transcription initiation site and the corresponding functional gene 2b in the murine coronavirus RNA genome. *J. Virol.* **63**, 3729–3736.
- Spaan, W., Delius, H., Skinner, M., Armstrong, J., Rottier, P., Smeekens, S., van der Zeijst, B. A. M., and Siddell, S. G. (1983). Coronavirus mRNA synthesis involves fusion of non-contiguous sequences. *EMBO J.* **2**, 1939–1944.
- van der Most, R. G., de Groot, R. J., and Spaan, W. J. M. (1994). Subgenomic RNA synthesis directed by a synthetic defective interfering RNA of mouse hepatitis virus: A study of coronavirus transcription initiation. **68**, 3656–3666.
- van Marle, G., Luytjes, W., van der Most, R. G., van der Straaten, T., and Spaan, W. J. M. (1995). Regulation of coronavirus mRNA transcription. *J. Virol.* **69**, 7851–7856.
- Winship, P. R. (1989). An improved method for directly sequencing PCR material using dimethyl sulfoxide. *Nucleic Acids Res.* **17**, 1266.
- Zhang, X., Liao, C. J., and Lai, M. M. C. (1994). Coronavirus leader RNA regulates and initiates subgenomic mRNA both in *trans* and in *cis*. *J. Virol.* **68**, 4738–4746.